ARS-2012-4574-ver9-Mishina_1P
Type: news

ANTIOXIDANTS & REDOX SIGNALING
Volume 00, Number 00, 2012

DOI: 10.1089/ars.2012.4574

NEWS & VIEWS

Can We See PIP_3 and Hydrogen Peroxide with a Single Probe?

AU1 ▶ Natalie M. Mishina,[1,2] Ivan Bogeski,[3] Dmitry A. Bolotin,[1] Markus Hoth,[3] Barbara A. Niemeyer,[3] Carsten Schultz,[4] Eleva V. Zagaynova,[2] Sergey Lukyanov,[1,2] and Vsevolod V. Belousov[1,2]

Abstract

A genetically encoded sensor for parallel measurements of phosphatidylinositol 3-kinase activity and hydrogen peroxide (H_2O_2) levels (termed PIP-SHOW) was developed. Upon elevation of local phosphatidylinositol 3,4,5-trisphosphate (PIP_3) concentration, the sensor translocates from the cytosol to the plasma membrane, while a ratiometric excitation change rapidly and simultaneously reports changes in the concentration of H_2O_2. The dynamics of PIP_3 and H_2O_2 generation were monitored in platelet-derived growth factor-stimulated fibroblasts and in T-lymphocytes after formation of an immunological synapse. We suggest that PIP-SHOW can serve as a prototype for many fluorescent sensors with combined readouts. *Antioxid. Redox Signal.* 00, 000–000.

Introduction

Fluorescent microscopy is a powerful method to study cell signaling *in vivo*. A wide spectrum of fluorescent proteins (FPs), FP-based sensors, and small-molecule chemical dyes allow visualization of many intracellular signaling events. Combinations of various fluorophores with distinct excitation and emission spectra in a single cell enable monitoring of multiple cellular processes simultaneously, usually termed multiparameter imaging (see Supplementary Data; Supplementary Data are available online at www.liebertonline.com/ars).

Phosphorylated forms of phosphoinositide lipids (PIPs) transduce signals *via* recruiting the PIP-binding domains that vary in their selectivity toward the number and position of phosphates of the inositol ring, allowing a fairly precise specificity of downstream signaling activation (8). One important lipid messenger is phosphatidylinositol 3,4,5-trisphosphate (PIP_3). Phosphatidylinositol 3-kinase (PI3K) phosphorylates AU3 ▶ $PI(4,5)P_2$ to PIP_3, while the lipid phosphatase PTEN reverses the phosphorylation (7). FPs fused with PIP_n-sensitive protein domains allow monitoring of PIP_n formation by translocation of the fluorescently labeled domain from the cytosol to the plasma membrane (PM) (8).

The global signaling activity of hydrogen peroxide (H_2O_2) is much less commonly addressed (3). H_2O_2 selectively and reversibly oxidizes a small population of cysteines that tend to be deprotonated at physiological pH (9). H_2O_2 production by NADPH oxidase (NOX)/dual oxidase (DUOX) enzymes and generation of PIP_3 by receptor tyrosine kinase activation can be highly cooperative: The NOX subunits p47 and p40 are

Innovation

Combinations of various fluorophores with distinct excitation and emission spectra in a single cell enable monitoring of multiple cellular processes simultaneously, usually termed multiparameter imaging. We successfully combined two different readouts in a single probe: ratiometric for hydrogen peroxide (H_2O_2) and translocation for phosphatidylinositol 3-kinase. The probe simultaneously detects the lipid messenger phosphatidylinositol 3,4,5-trisphosphate (PIP_3) and H_2O_2, showing that the two signals are highly cooperative. The performance of the sensor was tested in two cellular models, including immunological synapse formation of primary human T-cells, where we use it for kinetical measurements of two second messengers simultaneously. Making use of the subcellular localization of PIP_3 at the immune synapse, we are able to analyze H_2O_2 in subcellular domains with good resolution and a very good signal-to-noise ratio. Our data show as a proof of principle that different readouts can be easily combined in a single sensor, increasing a number of measured substances in a multiparameter imaging and minimizing a number of expression constructs.

[1]Shemyakin-Ovchinnikov Institute of Bioorganic Chemistry, Moscow, Russia.
[2]Nizhny Novgorod State medical academy, Nizhny Novgorod, Russia.
[3]Department of Biophysics, School of Medicine, Saarland University, Homburg, Germany.
[4]EMBL Heidelberg, Heidelberg, Germany. ◀ AU2

recruited to membranes by their PX domains that recognize products of PI3K activity and activate the oxidase activity (4). The subsequent H_2O_2 production then generates a positive feedback loop by oxidizing the active-site thiolate of PTEN, leading to an increased lifetime of PI3K products (5). To delineate the interplay of both signaling molecules more precisely, simultaneous detection of both PI3K activity and H_2O_2 levels would be necessary.

Genetically encoded sensor for H_2O_2, HyPer, is based on insertion of a yellow FP into regulatory domain of *Escherichia coli* H_2O_2 sensor OxyR (2). Upon oxidation and S-S bond formation within the OxyR domain, the excitation spectrum of HyPer changes in a ratiometric manner, proportionally decreasing its 420 nm and increasing its 500 nm excitation peak. Considering the interdependence of H_2O_2 and PI3K signaling, the simultaneous and spatially resolved measurement of both is desired in many cases. For this purpose, we have generated a sensor that reported changes in both PIP_3 and H_2O_2 concentration utilizing two different types of readout. Fusing HyPer with a PIP_3-sensitive PH domain should allow visualization of both PIP_3 generation (by translocation of the probe from the cytoplasm to the PM) and of H_2O_2 generation (by monitoring the excitation ratio 500/420 nm of HyPer).

Results, Discussion, and Future Directions

To generate a dual, PI3K and H_2O_2, sensor, we fused HyPer with a mutated PH domain (E41K) of Bruton's tyrosine kinase (BTK). The resulting reporter, named PIP-SHOW (PIP_3 and – SH Oxidation Watching) (Fig. 1A), emitted fluorescence signals in the expected wavelength range (500–550 nm) when expressed in NIH-3T3 fibroblasts. We then verified if the PIP-SHOW retained the ability of both domains, BTK-PH-E41K and HyPer, to respond to the respective stimuli, H_2O_2 and PIP_3. Addition of H_2O_2 resulted in the expected change in the probe's excitation ratio (Fig. 1B) similar to that of HyPer. Incubation of cells with 10 μM of a membrane-permeant photoactivatable version of PIP_3 (cgPIP_3/AM) and subsequent brief illumination with 405 nm light led to partial redistribution of the probe to the PM (Fig. 1C). Hence, both the translocation domain and the HyPer performed correctly.

To further characterize PIP-SHOW, we stimulated NIH-3T3 fibroblasts with platelet-derived growth factor (PDGF) and analyzed the fluorescence signals over time. Addition of PDGF initiated translocation of the probe to the PM reflecting PI3K activation and caused a significant change in the excitation ratio 500/420 nm, indicating generation of H_2O_2 (Fig. 2A; Supplementary Video S1). To quantify PI3K activity and

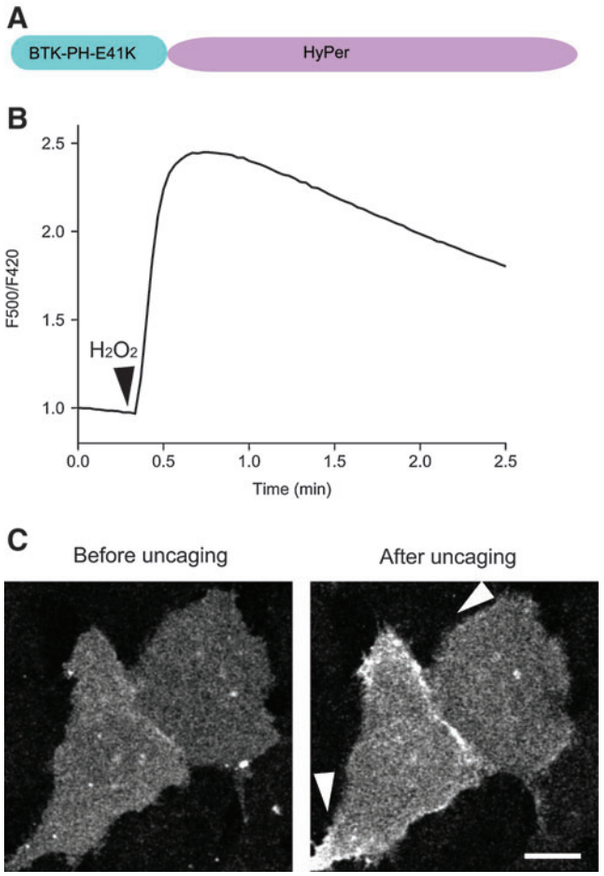

FIG. 1. PIP-SHOW reports changes in PIP_3 and H_2O_2 levels by two different types of readouts: translocation of the probe and excitation peaks ratio change, respectively. **(A)** PIP-SHOW consists of two parts, the PIP_3-sensitive PH domain of BTK and the H_2O_2 sensor HyPer. An E41K point mutation was introduced into the PH domain to increase sensitivity. **(B)** External H_2O_2 (50 μM) causes change in the sensor excitation ratio, F500/F420, in the cytoplasm of HeLa-Kyoto cell. **(C)** Photouncaging of synthetic PIP_3 causes redistribution of the probe to the PM domains. *Arrows* indicate zones of elevated PIP_3. Scale bar = 10 μm. (To see this illustration in color the reader is referred to the web version of this article at www.liebertonline.com/ars). H_2O_2, hydrogen peroxide; PIP, phosphatidylinositol phosphate; PIP_3, phosphatidylinositol 3,4,5-trisphosphate; PM, plasma membrane; BTK, Bruton's tyrosine kinase.

FIG. 2. Imaging PIP_3 and H_2O_2 with PIP-SHOW in NIH-3T3 cells stimulated with PDGF. (A) Widefield fluorescence images of PIP-SHOW–expressing NIH-3T3 cells at indicated time points (in minutes) after stimulation of the cells with 10 ng/ml PDGF. Upper row of images represent subcellular distribution of PIP-SHOW ratio reflecting changes in H_2O_2 level. Middle and lower rows of images show subcellular distribution of PIP-SHOW and changes in fluorescence intensity in each imaging channel. Individual cells are highlighted on the upper left corner ratio panel and numbered 1 to 4. Scale bar = 15 μm. The panel is representative of 20 cells from three experiments. **(B–E)** Time course of PI3K activation and H_2O_2 production by the cells 1 to 4 shown on **(A)**. Black lines reflect redistribution of PIP-SHOW to PM, red lines reflect H_2O_2 level changes in the cells. **(F)** Pretreatment of the NIH-3T3 cells with wortmannin (500 nM) abolished elevation of both PIP_3 and H_2O_2. Panel represents a typical time course of PIP_3 and H_2O_2 production by the cells pretreated with wortmannin. **(G)** The NOX inhibitor DPI (10 μM) inhibits H_2O_2 production but does not lead to a drop in PIP_3 levels. (To see this illustration in color the reader is referred to the web version of this article at www.liebertonline.com/ars). PI3K, phosphatidylinositol 3-kinase; PDGF, platelet-derived growth factor; DPI, diphenyleniodonium; NOX, NADPH oxidase.

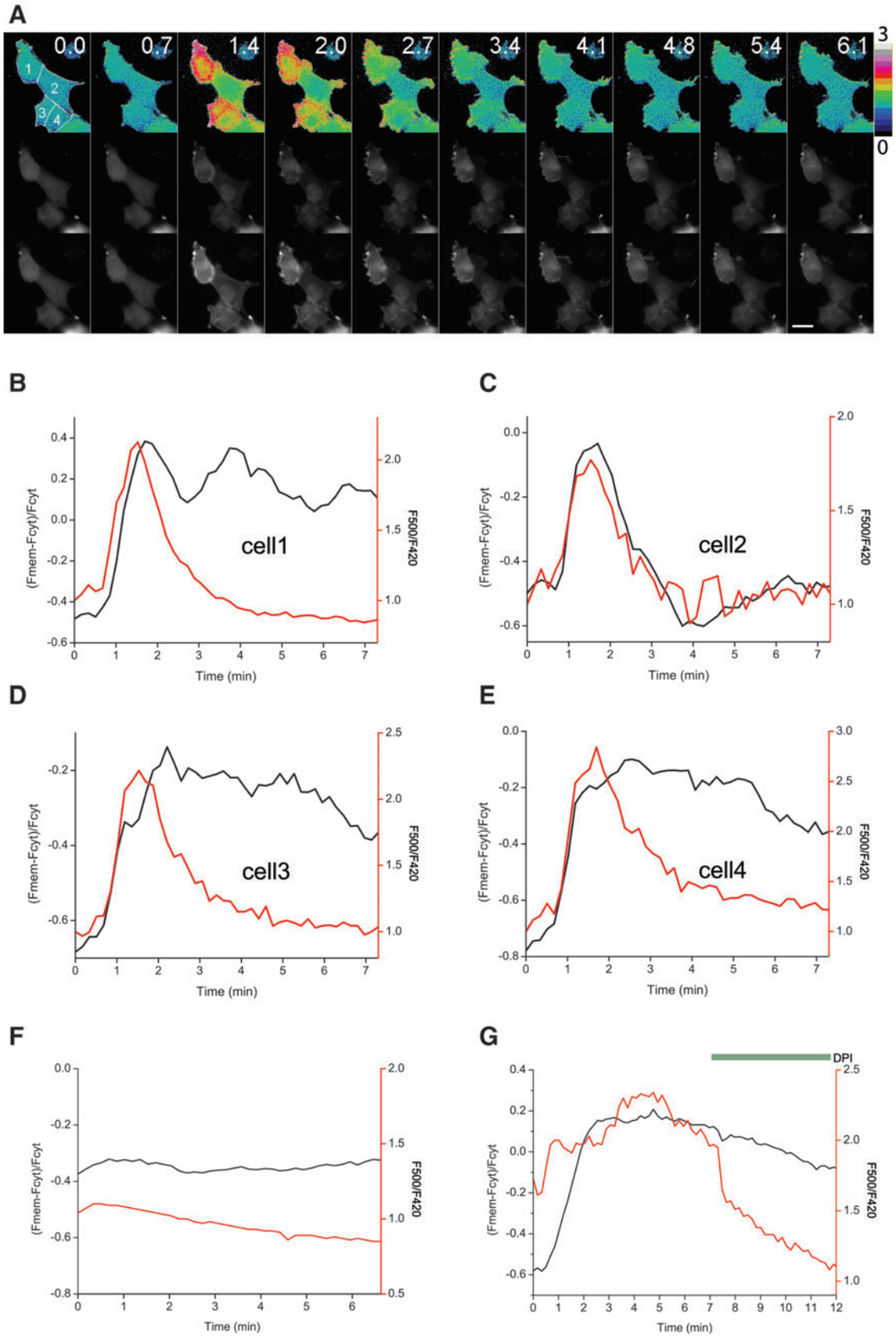
A
0.0
0.7
1.4
2.0
2.7
3.4
4.1
4.8
5.4
6.1
1
2
3
4
3
0
B
cell1
C
cell2
D
cell3
E
cell4
F
G
DPI
(Fmem-Fcyt)/Fcyt
F500/F420
Time (min)

H_2O_2 production in more detail, we analyzed their respective dynamics within single cells. Both signals were initially highly cooperative (Fig. 2B–E). Furthermore, Figure 2A–E showed that while both signals rose at similar times, PI3K accumulation reversed with a much slower time course, while H_2O_2 production was strictly transient. This indicates that both signals are not necessarily coupled for prolonged periods of time and highlights the importance of a dual sensor such as PIP-SHOW. This difference in kinetics could result from different sensitivities of the two domains comprising PIP-SHOW. However, this scenario is unlikely given their high sensitivity: BTK-PH-E41K domain was able to detect resting PIP_3 in the membrane of nonstimulated T-cells (see below) and the OxyR-RD domain of HyPer has extremely high reaction rates with H_2O_2 (10^7 $M^{-1}s^{-1}$), enabling intracellular H_2O_2 detection even in the presence of peroxiredoxins and glutathione peroxidases. PIP-SHOW does not completely translocate to the PM, and this allows comparison of the excitation ratio between the PM and the cytoplasm. Figure 2A shows that NIH-3T3 cells generate H_2O_2 in the vicinity of the PM, and that this H_2O_2 is unable to distribute uniformly throughout the cytoplasm. Because PI3K activity acts upstream of NOX/DUOX activation (4), we analyzed the effect of the PI3K inhibitor wortmannin on PI3K activity and H_2O_2 production, after stimulation with PDGF. Figure 2F shows that wortmannin prevented PI3K translocation but also inhibited H_2O_2 production. To further characterize PIP-SHOW, we inhibited NOX enzymes with diphenyleniodonium (DPI). Obviously, DPI led to a rapid drop in PIP-SHOW ratio reflecting decrease in H_2O_2 production (Fig. 2G). Because we did not observe a decrease in PIP_3 levels after DPI treatment, a potentially possible feedback loop between PI3K and NOX/DUOX activity *via* PTEN inhibition can be excluded.

Next, we utilized PIP-SHOW to study lipid and redox signaling events in the first phase of $CD4^+$human T helper (T_H) cell activation (Supplementary Data). Transient expression of PIP-SHOW in human T_H cells led to its localization within the cytoplasm as well as within the nucleus. However, a fraction of the probe showed membrane localization, indicating of pre-existing PI3K activity (Fig. 3A). Stimulation of T_H cells expressing PIP-SHOW with anti-CD3/CD28-coated beads led to establishment of stable contacts, immunological synapses (IS), between T_H cells and the beads (Fig. 3A; Supplementary Video S2). This was followed by a massive and immediate redistribution of PIP-SHOW to the IS indicative of locally elevated PIP_3 levels. The probe remained in the contact region for the duration of the experiment (up to 1 h). Notably, PI3K activity decreased at the rest of the PM of the activated cell as the ring-like fluorescence pattern disappeared immediately after IS formation (Fig. 3A). Furthermore, IS formation also led to a rapid elevation of H_2O_2, ~1 min after translocation of the PIP_3 sensor (Fig. 3; Supplementary Video S2). Interestingly, in most of the cells H_2O_2 production was highest in the region adjacent to the central synapse (Fig. 3E), implicating a ring-like localization of NOX/DUOX enzymes around the central IS. DPI quickly attenuated H_2O_2 production (Fig. 3F), suggesting that PM-localized NOX/DUOX are the source of H_2O_2. Similar to NIH-3T3 cells, there was no fast positive feedback loop between PI3K and NOX/DUOX activities, as we did not observe a decrease in PIP_3 upon addition of DPI (Fig. 3F). However, it is possible that the oxidant-induced decrease in phosphatase activity is only slowly reversible and acts in a long-term memory-like fashion. This might be the reason that a decrease in PIP_3 concentration was not detected in the time course of this experiment. Inhibition of PI3K by wortmannin, however, led to a rapid decrease in both PI3K activity and H_2O_2 production (Fig. 3G) as expected.

We demonstrated that the novel dual-parameter sensor PIP-SHOW is well suited for simultaneous monitoring of PIP_3 and H_2O_2 levels and can thereby serve as a prototype for indicators with combined readouts. The concept of a translocating domain fused to a ratiometric sensor is widely applicable to other combinations of intracellular signaling parameters as well. The second component of PIP-SHOW, HyPer, was designed and used to report H_2O_2 levels (2). Because HyPer is a protein of moderate size (~2 green fluorescent protein [GFP] molecules), it can be fused with subcellular localization tags. As HyPer is derived from a bacterially encoded protein, it is unlikely to interfere with other proteins and signaling pathways in mammalian cells. An important advantage of HyPer and therefore PIP-SHOW is the ratiometric response to H_2O_2, which is independent on the relative amount of the sensor, its redistribution, cell movement, or shape change. Indeed, in the theoretical case of intensiometric readout for H_2O_2 , it would be impossible to discriminate between PIP_3 and near-membrane H_2O_2 during PI3K activation and PIP-SHOW translocation. Thus, the ratiometric nature of HyPer is necessary to allow the simultaneous quantification of H_2O_2 during PI3K activity. In addition, we also showed that PIP-SHOW is combinable with RFP-based sensors, allowing synchronous measurements of an additional third parameter (Supplementary Fig. S1; Supplementary Data).

We validated PIP-SHOW using two cellular systems in which both PI3K and NOX/DUOX (reactive oxygen species [ROS]) were already shown to be important determinants of

FIG. 3. PIP-SHOW detects PI3K activity and H_2O_2 production in the human T_H cell upon IS formation. (A) Widefield fluorescence images of T_H cell forming a contact with anti-CD3/CD28–coated beads (added at timepoint zero). Numbers indicate time points in minutes. Upper row of the images represents transmitted light channel (beads are dense black); two next lower rows show distribution of the fluorescence sequentially excited at 420 and 505 nm; lowest row represents distribution of H_2O_2 represented by the 505/420 excitation ratio. Scale bar = 10 μm. **(B, C)** Time course of PI3K activation and H_2O_2 production in individual T_H cells. Black line reflects redistribution of PIP-SHOW to the IS; red line reflects H_2O_2 level changes in the cell. **(D)** Mean values of PI3K activity and H_2O_2 production in 28 T_H cells from three experiments and two donors. Error bars ± SEM. **(E)** Distribution of H_2O_2 between the IS and the cytoplasm in 44 cells from four experiments expressed as the ratio of the HyPer signal in the two subcompartments. Equal H_2O_2 concentration at the IS and in the cytoplasm is indicated by a ratio 1. **(F)** NOX inhibitor DPI (10 μM) reduces H_2O_2 production in the human T_H cell upon IS formation. **(G)** PI3K inhibitor wortmannin (500 nM) leads to a decrease in both PIP_3 and H_2O_2 levels. (To see this illustration in color the reader is referred to the web version of this article at www.liebertonline.com/ars). IS, immunological synapse; T_H, T helper; a.u..

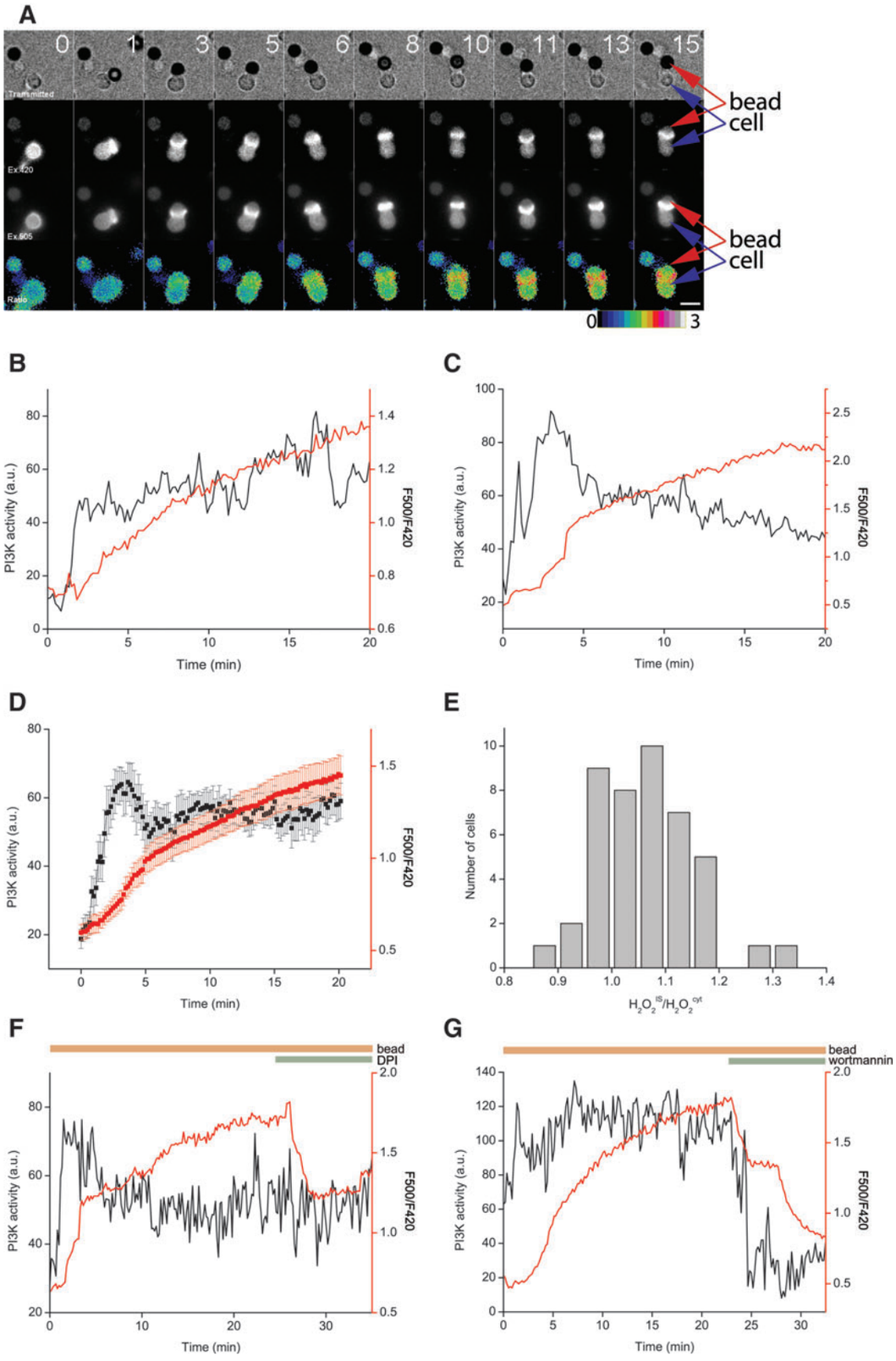
A
0
1
3
5
6
8
10
11
13
15
Transmitted
Ex.420
Ex.505
Ratio
bead
cell
bead
cell
0
3
B
PI3K activity (a.u.)
F500/F420
Time (min)
C
PI3K activity (a.u.)
F500/F420
Time (min)
D
PI3K activity (a.u.)
F500/F420
Time (min)
E
Number of cells
H2O2 IS/H2O2 cyt
F
bead
DPI
PI3K activity (a.u.)
F500/F420
Time (min)
G
bead
wortmannin
PI3K activity (a.u.)
F500/F420
Time (min)

several signaling pathways. Our results provide relevant information about the effectiveness of the sensor but also new information about the cooperative dynamics of the two signaling systems. While PDGF stimulated fibroblasts are a well-documented experimental model to study lipid and redox signaling, not much was known about the role of ROS and their interaction with PI3K and, respectively, PIP_3 in human T_H cells.

In both cellular systems, H_2O_2 and PIP_3 demonstrated a high degree of synchronicity, particularly in the initial phase after stimulation (see Figs. 2 and 3). In fibroblasts, however, the decrease in H_2O_2 was accompanied by decrease in PIP_3 only in a fraction of the cells. In polarized T cells, on the other hand, the PI3K activity rapidly redistributed and increased at the IS and decreased in the rest of the PM. The H_2O_2 distribution demonstrated a higher degree of heterogeneity: whereas in most of the cells highest H_2O_2 levels were detected at the IS, in some H_2O_2 was more evenly distributed (Fig. 3E). Nevertheless, in most cases the source of H_2O_2 was visibly associated with either the PM or, more specifically, the IS. Interestingly, in contrast to fibroblasts, PI3K activity in the stimulated T_H cells started before H_2O_2 production was detectable with HyPer (Figs. 2 and 3). More physiological studies are needed to determine the functional role of local ROS microdomains close to the IS not only in T_H but also in other immune cells.

PIP_3 concentration at the PM is a result of the concerted action of the PI3-kinases and lipid phosphatases. The latter contain, similar to protein tyrosine phosphatases, thiolates in the active site, rendering them redox sensitive. H_2O_2 was shown to oxidize the lipid phosphatase PTEN, enabling positive feedback loop in the phosphorylation cascade. We would therefore expect to see a decrease in PIP_3 concentration upon elimination of H_2O_2. The kinetics of PIP-SHOW disulphide reduction should be similar to the reduction of the phosphatases. To our surprise, in both experimental models we did not see an effect of NOX inhibition on the PIP_3 content. While the HyPer signal (H_2O_2) decreased rapidly upon addition of DPI, the localization of the PH domain did not change, indicating that PIP_3 concentrations did not decrease significantly. A possible explanation is that in strongly stimulated cells, PI3K activity is dominating over phosphatases activity in such a way that inhibition of the phosphatases (at least lipid phosphatases) by H_2O_2 does not shift the equilibrium significantly. Another interpretation might be an increased sensitivity of the probe to PIP_3 due to the E41K mutation that prevents retrograde translocation of the sensor. However, this explanation appears unlikely because inhibition of PI3K by wortmannin led to rapid redistribution of the probe from PM to cytoplasm, implicating a high lipid phosphatase activity.

In summary, we successfully combined two different readouts in a single probe. In fact, a variety of translocation-based sensor domains are suitable to be fused with any ratiometric indicator regardless whether it is single fluorophore or a Forster resonance energy transfer pair. Ratiometric sensors can serve as the fluorescence tags instead of conventional FPs, and they can provide additional read-out parameters, such as 2nd messenger concentrations in time-lapse imaging experiments. Obvious other benefits are that only a small part of the usable spectra is occupied and additional colors may be used for other sensors in a multiparameter imaging setup. Most importantly, only one expression construct is needed for the dual-parameter readout, which makes the relative quantification and the interpretation of the results much easier.

Notes

Materials used

H_2O_2, DPI, EGF, and PDGF-BB were purchased from Sigma. Dulbecco-phosphate-buffered saline, Dulbecco's modified Eagle's medium (DMEM), Opti–minimal essential medium (MEM), MEM, fetal calf serum (FCS), and FuGene6 transfection reagent were from Invitrogen. Glass-bottomed dishes were fromMatTec. NIH-3T3 cells were from ATCC. HeLa-Kyoto cell line was provided by EMBL. Encyclo polymerase chain reaction (PCR) kit and HyPer expression vectors were from Evrogen. Restriction endonucleaseswere from SibEnzyme.

DNA constructs

To make PIP-SHOW, the PH-domain coding region of BTK was amplified from pEGFP-BtkPH encoding vector using the primers 5′-ATCCGCTAGCATGGCCGCAGTGATTCTG G AGA-3′ and 5′-CGGTGGATCCCCGTTCTCCAAAATTT GG CAGCCCA-3′. The PCR product was digested with *Nhe*I and *Bam*HI and cloned into pHyPer-dMito vector (Evrogen) in place of double MTS-coding sequence. It has been shown that E41K mutation increases the affinity of the BTK-PH to PIP_3 (1). To introduce E41K mutation, site-directed mutagenesis of Btk PH-domain was applied using the PCR overlap extension procedure with the primers 5′-CTCCTACTATA AGTATGACTT TGA-3′ and 5′-TCAAAGTCATACTTATAG TAGGAG-3′. All constructs were confirmed by sequence analysis.

Cell culture and transfection

NIH-3T3 cells were cultured in DMEM supplemented with 10% FCS at 37°C in an atmosphere containing 95% air and 5% CO_2. Cells were split every 2nd day and seeded on glass bottom dishes. Twenty-four hours later cells were transfected by the mixture of vector DNA and FuGene6 transfection reagent according to the manufacturer recommendations.

Human T_H cells were isolated from leukocyte reduction filters from healthy blood donors. First, peripheral blood lymphocytes (PBLs) were purified by a density gradient centrifugation at 450 *g* for 30 min at room temperature (Ficoll-Paque PLUS, Amersham Biosciences), while the remaining red blood cells were removed using a lysis buffer (155 m*M* NH4Cl, 10 m*M* KHCO3, and 0.1 m*M* EDTA [pH 7.3]). PBLs were resuspended in PBS buffer containing 0.5% BSA, and $CD4^+$ T_H cells were negatively isolated using $CD4^+$ negative isolation kit (Invitrogen). Naïve T_H cells were transfected ~ 4 h after isolation using Nucleofector II electroporator (Lonza, program U-014) and Human T cell Nucleofector kit (Lonza) according to manufacturer's instructions. Per one million cells 1 μg DNA was electroporated 24 to 48 h after transfection, and the cells were attached (~10 min, 37°C) to poly-l-ornithine–coated (0.1 mg/ml) glass coverslips, and imaged. ◀ AU4

Imaging

The T_H cells were imaged at 37°C using a Zeiss Cell Observer HS widefield microscope equipped with a 40× Fluar oil lense (N.A. 1.3), an LED fluorescence lamp (Colibri, Zeiss),

an and a photometric evolve: 512 EMCCD camera at binning 1×1. Filters were a CFP, YFP dualband pinkel set (55HE, Zeiss). Fluorescence was recorded using excitation at 420 and 505 nm and emission at 515 nm. NIH-3T3 cells were imaged using Leica 6000 widefield microscope equipped with an HCX PL APO lbd.BL 63×1.4NA oil objective and an environmental chamber. Fluorescence was excited sequentially *via* 427/10 and 504/12 band-pass excitation filters. Emission of the probe was collected every 10 or 30 s using a 525/50 band-pass emission filter. After three to five images were acquired, 10 ng/ml PDGF was added.

cgPI(3,4,5)P_3/AM treatment and uncaging

AU3 ▶ cgPI(3,4,5)P_3/AM (6) was dissolved in DMSO at stock concentration of 10 m*M*. Just before applying to cells it was mixed with 10% pluronic/DMSO solution (Invitrogen) in 1:1 ratio to facilitate cell entry. cgPI(3,4,5)P_3/AM was used on cells in a concentration of 10 μM. Uncaging and imaging were performed on Carl Zeiss LSM 510-META confocal microscope, equipped with environment control box (37°C, 0% CO_2), using HCX PL APO lbd. 60×1.4NA oil objective. Cells were preincubated with cgPI(3,4,5)P_3/AM 2 h before uncaging in the imaging medium. For uncaging, cells were illuminated with 405 nm laser (7%) every 10 s. Imaging of PIP_3-SHOW was done using 488 nm laser excitation (5%) with 10 s time resolution.

Time series processing

Time series were analyzed using ImageJ software. For H_2O_2 dynamics calculation, stacks corresponding to 420 and 500 nm excitation peaks of PIP-SHOW were converted to 32 bit after background subtraction. 420-nm stack was thresholded to remove pixel values from background (Not-a-Number function). A 500-nm stack was divided by the corresponding 420-nm stack frame by frame. The resulting stack was depicted in pseudocolors using a "ratio" lookup table. Time course of PIP-SHOW fluorescence was calculated for regions of interest (ROI) inside the imaged cell. The anti-CD3/CD28-coated beads used for T cell stimulation are fluorescent in both channels; however, that fluorescence does not change. The F500/F420 ratio of the beads was set as 1 and all the ratio stacks were normalized to this value. For PI3K activity monitoring, different quantification strategies were applied for the NIH-3T3 cells and for the lymphocytes. For NIH-3T3 cells, two ROI were set up for each cell corresponding to the cytoplasm and to the AU3 ▶ PM. Distribution of the probe was calculated as Value = (Fmem AU3 ▶ – Fcyt)/Fcyt. Application of this equation to either 420 or 500 nm channels gives similar results. Since T_H cells are highly motile, it turns to be very time consuming to draw ROIs representing IS and the cytoplasm manually for each frame. We therefore utilized different strategy based on bright pixels count. During accumulation of the probe at the IS, the percentage of high-intensity pixels increased. Therefore, if the low- and medium-intensity pixels are thresholded and set to "Not-a-Number," dynamics of the mean value of the remaining bright pixels shows dynamics of PI3K activity in the IS. However, in case of PIP-SHOW the brightness of the probe in either channel depends also on H_2O_2. The influence of H_2O_2 can be removed by dividing each frame in the stack by the mean value (in the same frame) of the ROI drawn in the cytoplasm of the cell. To enable this procedure, we designed a simple ImageJ plugin named "Divide by ROI" (Supplementary Data). Being applied to the 420-nm stack (420 nm channel brightness is less dependent on H_2O_2 compared to 500 nm channel), the plugin divides each frame by the mean value of the ROI in the same frame. After that, 32-bit images were thresholded leaving upper 50% (by intensity) of the pixels visible. Mean intensity profile over time gives PI3K dynamics in relative units.

Acknowledgments

This work was supported by the Russian Foundation for Basic Research (10-04-01561-a, V.V.B; 11-04-12187-ofi, S.L); the Ministry of Education and Science of the Russian Federation (16.512.11.2139, 16.740.11.0367); the Measures to Attract Leading Scientists to Russian Educational Institutions program (11.G34.31.0017 to S.L); ESF (TraPPs, C.S); DFG (to I.B. (BO 3643/2-1), to C.S. Schu 943/7-1; SFB 894 and GK 845 to M.H.; NI671/3-1, SFB 894; and GK 1326 to B.A.N.

References

1. Baraldi E, Djinovic Carugo K, Hyvonen M, Surdo PL, Riley AM, Potter BV, O'Brien R, Ladbury JE, and Saraste M. Structure of the PH domain from Bruton's tyrosine kinase in complex with inositol 1,3,4,5-tetrakisphosphate. *Structure* 7: 449–460, 1999.
2. Belousov VV, Fradkov AF, Lukyanov KA, Staroverov DB, Shakhbazov KS, Terskikh AV, and Lukyanov S. Genetically encoded fluorescent indicator for intracellular hydrogen peroxide. *Nat Methods* 3: 281–286, 2006.
3. D'Autreaux B and Toledano MB. ROS as signalling molecules: mechanisms that generate specificity in ROS homeostasis. *Nat Rev Mol Cell Biol* 8: 813–824, 2007.
4. Kanai F, Liu H, Field SJ, Akbary H, Matsuo T, Brown GE, Cantley LC, and Yaffe MB. The PX domains of p47phox and p40phox bind to lipid products of PI(3)K. *Nat Cell Biol* 3: 675–678, 2001.
5. Kwon J, Lee SR, Yang KS, Ahn Y, Kim YJ, Stadtman ER, and Rhee SG. Reversible oxidation and inactivation of the tumor suppressor PTEN in cells stimulated with peptide growth factors. *Proc Natl Acad Sci U S A* 101: 16419–16424, 2004.
6. Mentel M, Laketa V, Subramanian D, Gillandt H, and Schultz C. Photoactivatable and cell-membrane-permeable phosphatidylinositol 3,4,5-trisphosphate. *Angew Chem Int Ed Engl* 50: 3811–3814.
7. Tamguney T and Stokoe D. New insights into PTEN. *J Cell Sci* 120: 4071–4079, 2007.
8. Varnai P and Balla T. Live cell imaging of phosphoinositide dynamics with fluorescent protein domains. *Biochim Biophys Acta* 1761: 957–967, 2006.
9. Winterbourn CC. Reconciling the chemistry and biology of reactive oxygen species. *Nat Chem Biol* 4: 278–286, 2008.

Abbreviations Used

BTK = Bruton's tyrosine kinase
DMEM = Dulbecco's modified Eagle's medium
DMSO =
DPI = diphenyleniodonium
DUOX = dual oxidase
FCS = fetal calf serum
FP = fluorescent protein
GFP = green fluorescent protein
H_2O_2 = hydrogen peroxide
IS = Immunological synapse
NOX = NADPH oxidase
PBLs = peripheral blood lymphocytes

◀ AU3

Abbreviations Used (Cont.)

PCR = polymerase chain reaction
PDGF = platelet-derived growth factor
PI3K = phosphatidylinositol 3-kinase
PIP = phosphatidylinositol phosphate
PIP_3 = phosphatidylinositol 3,4,5-trisphosphate
PM = plasma membrane
AU3 ► PTEN =
ROI = regions of interest
ROS = reactive oxygen species
T_H = T helper

Address correspondence to:
Dr. Vsevolod V. Belousov
Shemyakin-Ovchinnikov Institute of Bioorganic Chemistry
Miklukho-Maklaya 16/10
Moscow 117997
Russia

E-mail: vsevolod.belousov@gmail.com

Date of first submission to ARS Central, February 17, 2012; date of acceptance, February 18, 2012.

Supplementary Data

Multiparameter imaging

Combinations of various fluorophores with distinct excitation and emission spectra in a single cell enable monitoring of multiple cellular processes simultaneously, usually termed "multiparameter imaging" (MI) (5, 20). Typical readouts of the fluorescent probes are (i) changes in emission brightness (14, 22); (ii) ratiometric changes between two excitation or emission peaks (1, 2, 8, 12), especially when Forster resonance energy transfer probes are involved (4, 5, 10, 13, 23); and (iii) translocation of the probe from one to another cellular compartment (20, 24). The combination of these modalities should provide even more opportunities for MI in living cells. So far, only very few examples of dual parameter fluorescent sensors have been reported (4).

Combining red fluorescent readout with PIP-SHOW imaging

MI by PIP-SHOW does not use the entire available visible spectra for life cell imaging. Therefore, we combined measurements of PIP-SHOW with a translocation probe (C2-mRFP) to detect changes in intracellular calcium ions $[Ca^{2+}]_i$ (15, 25). C2 domain binds phosphatidylserine upon elevation of $[Ca^{2+}]_i$ translocating from the cytoplasm to the plasma membrane (PM). Therefore, by monitoring C2-mRFP

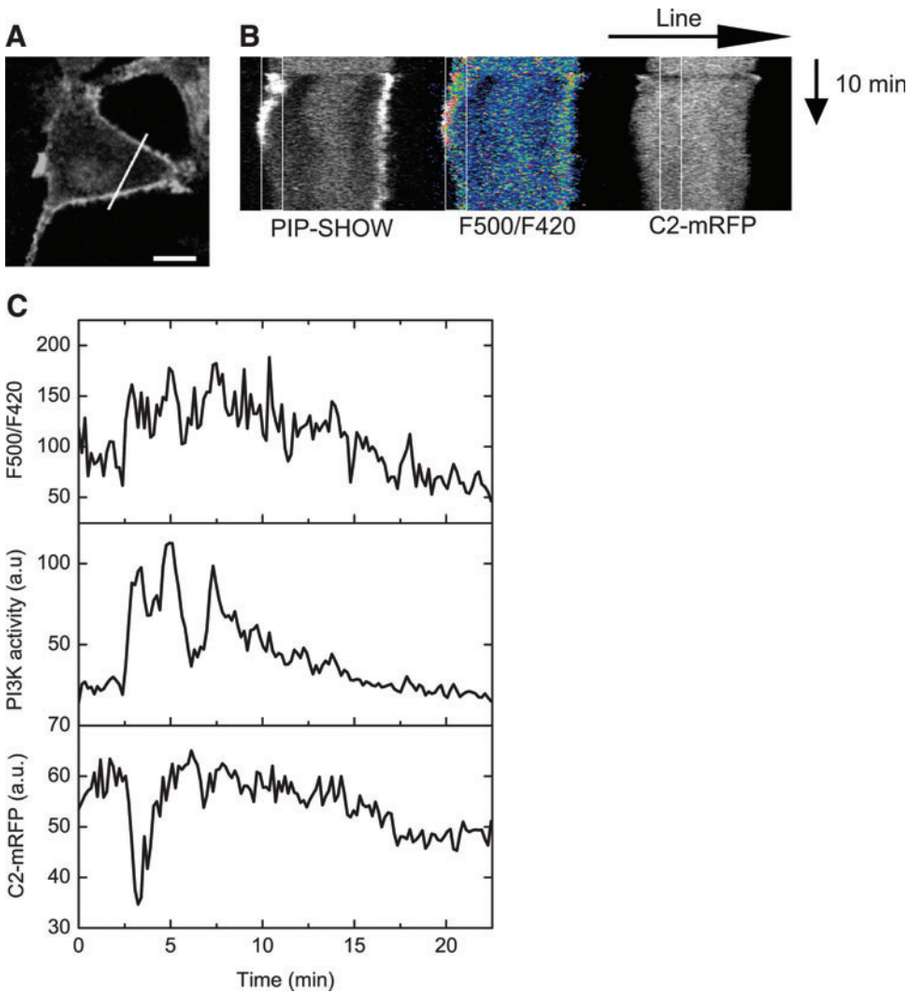

SUPPLEMENTARY FIG. S1. Kymogram of simultaneous imaging of PIP_3, H_2O_2 and Ca^{2+} in NIH-3T3 cells expressing PIP-SHOW and C2-mRFP. (A) A line across the cell was chosen to build kymogram from the time stack. Scale bar = 10 μm. **(B)** Kymograms of PIP_3 (PIP-SHOW), H_2O_2 (F500/F420), and Ca^{2+} (C2-mRFP) dynamics along the line in time. ROIs were chosen as vertical lines of 20-pixel thickness to measure profiles of fluorescence changes with time. PIP_3 and H_2O_2 were measured in the ROI that includes plasma membrane. Ca^{2+} dynamics was measured in the ROI that includes cytoplasm (C2-mRFP drop upon Ca^{2+} elevation). **(C)** Changes in PIP_3, H_2O_2, and Ca^{2+} along the selected ROIs in time. H_2O_2, hydrogen peroxide; ROI, regions of interest; PIP, phosphatidylinositol phosphate.

SUPPLEMENTARY VIDEO S1. PIP-SHOW reports PI3K activity and H_2O_2 levels change by two different types of readouts: translocation of the probe and excitation peaks ratio change. See legend of Figure 2 in the main text for details. PI3K, phosphatidylinositol 3-kinase; H_2O_2, hydrogen peroxide; PIP, phosphatidylinositol phosphate.

SUPPLEMENTARY VIDEO S2. PIP-SHOW detects PI3K activity and H_2O_2 production in the human T_H cell upon IS formation. See legend of Figure 3 in the main text for details. IS, immunological synapse; T_H, T helper.

translocation, it was possible to track $[Ca^{2+}]_i$ dynamics. We co-expressed PIP-SHOW and C2-mRFP in NIH-3T3 fibroblasts and stimulated the cells with platelet-derived growth factor. We were able to monitor three parameters (hydrogen peroxide $[H_2O_2]$, phosphatidylinositol 3,4,5-trisphosphate $[PIP_3]$, and cytosolic $[Ca^{2+}]_i$) in parallel (Supplementary Fig. S1). Translocation of C2-mRFP showed rapid and transient elevation of $[Ca^{2+}]_i$. By analyzing PIP-SHOW translocation and F500/F420 ratio, we were able to demonstrate that elevations of PIP_3 and H_2O_2 occur at a similar time scale compared to $[Ca^{2+}]_i$ increases. However, both PIP_3 and H_2O_2 signals decayed much slower than $[Ca^{2+}]_i$.

AU5 ► *Lipid and redox signaling in TCR* activation

PIP_3 signaling plays a key role in T cell activation (16, 21, AU6 ► 26), and TCR stimulation leads to generation of reactive oxygen species (ROS) (9, 18). T helper (T_H) cells are activated through the interaction of their TCRs, together with co-stimulatory receptors (*i.e.*, CD28), with the major histocompatibility complex on the surface of antigen-presenting cells, thereby forming an immunological synapse (IS) (11). In *in vitro* studies, IS formation can be mimicked by incubation of cells with beads coated with anti-CD3/anti-CD28 antibodies (17). It has been shown that IS formation leads to a strong activation of phosphatidylinositol 3-kinase (PI3K) and PIP_3 elevation both at the IS and throughout rest of PM (6, 7). Although formation of ROS has been shown to appear downstream of TCR signaling, real-time dynamics, quantification, and localization of H_2O_2 during IS formation are very difficult to assess. Previous work demonstrated ROS production by T_H cells stimulated with soluble agonists using the AU6 ► fluorescent redox-sensitive dye DCF (9). However, DCF derivatives have many disadvantages, such as photoinduced ROS production and lack of specificity toward different species of ROS (3, 19). Moreover, stimulation with soluble TCR cross-linkers does not lead to T cell polarization and IS formation. We therefore studied dynamics of both PI3K and H_2O_2 during IS formation.

References

1. Belousov VV, Fradkov AF, Lukyanov KA, Staroverov DB, Shakhbazov KS, Terskikh AV, and Lukyanov S. Genetically encoded fluorescent indicator for intracellular hydrogen peroxide. *Nat Methods* 3: 281–286, 2006.
2. Berg J, Hung YP, and Yellen G. A genetically encoded fluorescent reporter of ATP:ADP ratio. *Nat Methods* 6: 161–166, 2009.
3. Bonini MG, Rota C, Tomasi A, and Mason RP. The oxidation of 2′,7′-dichlorofluorescin to reactive oxygen species: a self-fulfilling prophesy? *Free Radic Biol Med* 40: 968–975, 2006.
4. Brumbaugh J, Schleifenbaum A, Gasch A, Sattler M, and Schultz C. A dual parameter FRET probe for measuring PKC and PKA activity in living cells. *J Am Chem Soc* 128: 24–25, 2006.
5. Carlson HJ and Campbell RE. Genetically encoded FRET-based biosensors for multiparameter fluorescence imaging. *Curr Opin Biotechnol* 20: 19–27, 2009.
6. Costello PS, Gallagher M, and Cantrell DA. Sustained and dynamic inositol lipid metabolism inside and outside the immunological synapse. *Nat Immunol* 3: 1082–1089, 2002.
7. Harriague J and Bismuth G. Imaging antigen-induced PI3K activation in T cells. *Nat Immunol* 3: 1090–1096, 2002.
8. Hung YP, Albeck JG, Tantama M, and Yellen G. Imaging cytosolic NADH-NAD(+) redox state with a genetically encoded fluorescent biosensor. *Cell Metab* 14: 545–554.
9. Kwon J, Shatynski KE, Chen H, Morand S, de Deken X, Miot F, Leto TL, and Williams MS. The nonphagocytic NADPH oxidase Duox1 mediates a positive feedback loop during T cell receptor signaling. *Sci Signal* 3: ra59.
10. Mank M, Reiff DF, Heim N, Friedrich MW, Borst A, and Griesbeck O. A FRET-based calcium biosensor with fast signal kinetics and high fluorescence change. *Biophys J* 90: 1790–1796, 2006.
11. Monks CR, Freiberg BA, Kupfer H, Sciaky N, and Kupfer A. Three-dimensional segregation of supramolecular activation clusters in T cells. *Nature* 395: 82–86, 1998.
12. Nagai T, Sawano A, Park ES, and Miyawaki A. Circularly permuted green fluorescent proteins engineered to sense Ca^{2+}. *Proc Natl Acad Sci U S A* 98: 3197–3202, 2001.
13. Nagai T, Yamada S, Tominaga T, Ichikawa M, and Miyawaki A. Expanded dynamic range of fluorescent indicators for Ca(2+) by circularly permuted yellow fluorescent proteins. *Proc Natl Acad Sci U S A* 101: 10554–10559, 2004.
14. Nakai J, Ohkura M, and Imoto K. A high signal-to-noise Ca(2+) probe composed of a single green fluorescent protein. *Nat Biotechnol* 19: 137–141, 2001.
15. Oancea E and Meyer T. Protein kinase C as a molecular machine for decoding calcium and diacylglycerol signals. *Cell* 95: 307–318, 1998.
16. Okkenhaug K and Vanhaesebroeck B. PI3K in lymphocyte development, differentiation and activation. *Nat Rev Immunol* 3: 317–330, 2003.
17. Quintana A, Schwindling C, Wenning AS, Becherer U, Rettig J, and Schwarz EC, Hoth M. T cell activation requires mitochondrial translocation to the immunological synapse. *Proc Natl Acad Sci U S A* 104: 14418–14423, 2007.
18. Reth M. Hydrogen peroxide as second messenger in lymphocyte activation. *Nat Immunol* 3: 1129–1134, 2002.
19. Rota C, Chignell CF, and Mason RP. Evidence for free radical formation during the oxidation of 2′-7′-dichlorofluorescin to the fluorescent dye 2′-7′-dichlorofluorescein by horseradish

peroxidase: possible implications for oxidative stress measurements. *Free Radic Biol Med* 27: 873–881, 1999.
20. Schultz C, Schleifenbaum A, Goedhart J, and Gadella TW, Jr. Multiparameter imaging for the analysis of intracellular signaling. *Chembiochem* 6: 1323–1330, 2005.
21. Smith-Garvin JE, Koretzky GA, and Jordan MS. T cell activation. *Annu Rev Immunol* 27: 591–619, 2009.
22. Tian L, Hires SA, Mao T, Huber D, Chiappe ME, Chalasani SH, Petreanu L, Akerboom J, McKinney SA, Schreiter ER, Bargmann CI, Jayaraman V, Svoboda K, and Looger LL. Imaging neural activity in worms, flies and mice with improved GCaMP calcium indicators. *Nat Methods* 6: 875–881, 2009.
23. Tsutsui H, Karasawa S, Okamura Y, and Miyawaki A. Improving membrane voltage measurements using FRET with new fluorescent proteins. *Nat Methods* 5: 683–685, 2008.
24. VanEngelenburg SB and Palmer AE. Fluorescent biosensors of protein function. *Curr Opin Chem Biol* 12: 60–65, 2008.
25. Yu HY and Bement WM. Control of local actin assembly by membrane fusion-dependent compartment mixing. *Nat Cell Biol* 9: 149–159, 2007.
26. Zhang TT, Li H, Cheung SM, Costantini JL, Hou S, Al-Alwan M, and Marshall AJ. Phosphoinositide 3-kinase-regulated adapters in lymphocyte activation. *Immunol Rev* 232: 255–272, 2009.

AUTHOR QUERY FOR ARS-2012-4574-VER9-MISHINA_1P

AU1: Please review all authors' surnames for accurate indexing citations.
AU2: Please expand EMBL in author's affiliation 4.
AU3: Please define PTEN, DMSO, Fmem, Fcyt, and a.u.
AU4: Please expand BSA and SEM.
AU5: Please expand TCR.
AU6: Please define TCR and DCF.